Dalton Transactions

Squeezing the box: Isoreticular contraction of pyrene-based linker in a Zr-based metal–organic framework for Xe/Kr separation

Journal:	*Dalton Transactions*
Manuscript ID	DT-COM-02-2020-000546.R1
Article Type:	Communication
Date Submitted by the Author:	12-Mar-2020
Complete List of Authors:	Maldonado, Rodrigo; Northwestern University, Chemistry Zhang, Xuan; Northwestern University, Hanna, Sylvia; Northwestern University, Chemistry Gong, Xinyi; Northwestern University, Chemistry Gianneschi, Nathan; Northwestern University, Chemistry; University of California, San Diego, Chemistry and Biochemistry Hupp, Joseph; Northwestern University, Chemistry Farha, Omar; Northwestern University, Chemistry

COMMUNICATION

Squeezing the box: Isoreticular contraction of pyrene-based linker in a Zr-based metal–organic framework for Xe/Kr separation

isoReceived 00th January 20xx,
Accepted 00th January 20xx

DOI: 10.1039/x0xx00000x

Rodrigo R. Maldonado, Xuan Zhang, Sylvia Hanna, Xinyi Gong, Nathan C. Gianneschi, Joseph T. Hupp, Omar K. Farha

Isoreticular synthesis is a powerful tool to enhance specific attributes of a metal-organic framework (MOF). While the isoreticular expansion of MOF structure are prevalent in the literature, the compression of a topology holds great promise for separations due to the contracted pore apertures and/or cavities. Herein, we report the synthesis, characterization and Xe/Kr separation capability of a new Zr-based MOF, NU-1106, connected by the tetratopic linker 1,3,6,8-pyrene tetracarboxylate, which exhibits a compressed *ftw* topology compared to the extended ones reported previously. NU-1106 showed selective uptake of Xenon over Krypton, providing the potential for use for separations.

Molecular (and atomic) separations constitute important processes industrially for the extraction and purification of a variety of different gases and chemicals. It is estimated that industrial separations make up approximately 15% of the total US energy consumption (the equivalent of $15x10^{15}$ BTU), the majority of which is due to distillations.[1] In particular, distillations are thermally-driven processes that separate by differences in boiling points for the components in the mixture. For components naturally found in the gas-phase at ambient temperatures, distillations often occur at temperatures much lower than room-temperature to condense and then separate gases.[1, 2] Though cryogenic distillations produce high yields of gas at very high purities, achieving and maintaining the low temperatures is an energetically-intensive process. One such process that could benefit from an alternative approach is the separation of radioactive isotopes produced in nuclear plants, particularly xenon and krypton.[3] Due to their similar sizes (kinetic diameters of 3.96 and 3.60 Å) and chemical inertness, the best alternative would exploit the polarizability of Xe over Kr in an adsorption process.[4, 5]

Metal-organic frameworks (MOFs) show potential for alternative use in the more energy-efficient adsorption-based separation processes. Organic linkers coordinate to metal nodes to form three-dimensional, crystalline, and porous materials known as MOFs.[6, 7] Altering specific combinations of linkers and nodes - as well as the synthetic conditions - modify the topology and adjust a MOF's selective interactions with guest molecules.[8, 9]

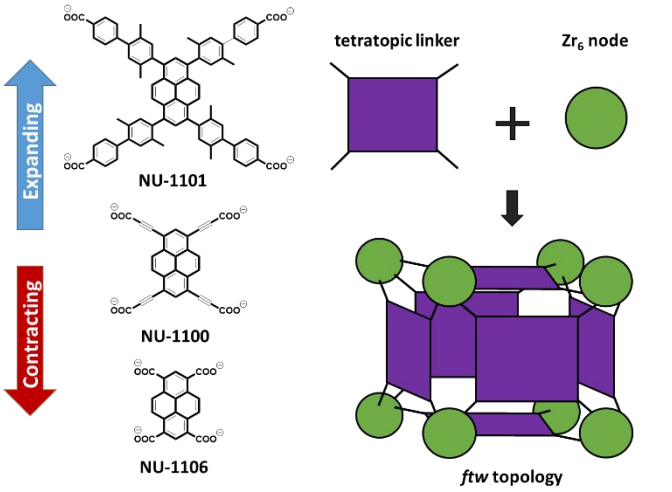

Figure 1. Designing *ftw* MOFs. NU-110X series uses tetratopic linkers of different lengths.

[a] *Department of Chemistry and International Institute of Nanotechnology, Northwestern University, 2145 Sheridan Road, Evanston, Illinois 60208*

Electronic Supplementary Information (ESI) available: [details of any supplementary information available should be included here]. See DOI: 10.1039/x0xx00000x

For nearly two decades, MOFs have been evaluated for a variety of potential applications ranging from catalysis,[10, 11] water remediation,[12, 13] and enzyme encapsulation.[14-16] Advancements in both their robustness and tunability have made MOFs optimal scaffolds for studying gas-phase separations, especially the developments made for isoreticular synthesis.[8] To clarify, isoreticular synthesis alters either the linker or node of a known MOF to form the same topology but differs a specific moiety to change a MOF's porosity and/or functionality. One notable example of isoreticular synthesis is the development of MOFs with *ftw* topology, as shown in the **NU-110X** (X = 0-5) series (**Figure 1**). **NU-110X** MOFs form cubic cages structured around twelve-connected Zr_6-nodes.[7, 17] Tetratopic pyrene linkers tether to four nodes to form distinct diamond-shaped apertures at each edge of the cage, thereby restricting MOF flexibility. In addition, Zr-based MOFs are well-known to coordinate strongly to carboxylate groups, leading to

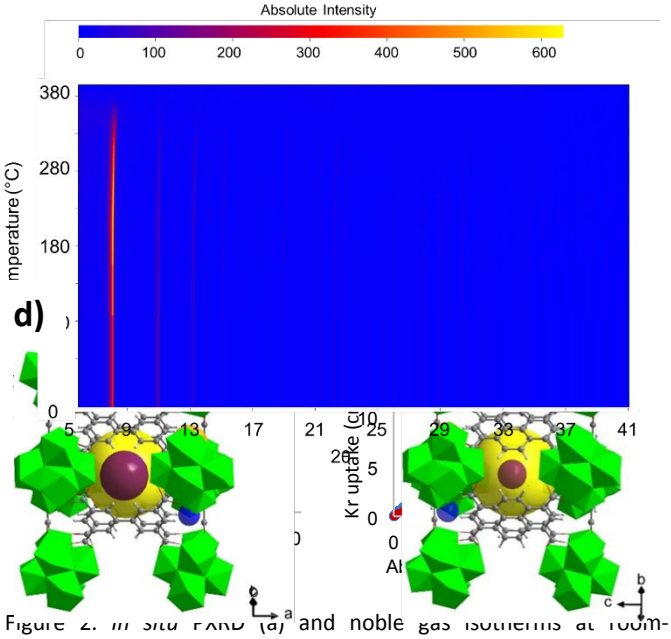

Figure 2. *In situ* PXRD (a) and noble gas isotherms at room-temperature (b,c). PXRD shows the loss of crystallinity after 350 °C. NU-1106 (blue) shows greater adsorption as opposed to the biphenyl version (red) of the *ftw* MOF. (d) Simulated ideal structures of NU-1106 (right) and Zr-BPTC version (left). The MOFs are labeled as follows: Zr_6 node (green polyhedra), carbon (gray spheres), hydrogen (white spheres), pore diameter (yellow sphere), large pore aperature (magenta sphere), small pore aperature (blue sphere). The model for NU-1106 was based from reported Zr-BPTC structure.

robust materials.[18, 19] Previous work focused extensively on the isoreticular expansion of the framework via extension of organic linkers, to increase the MOF surface area and improve the storage capacity.[20-22] Strategies for isoreticular synthesis previously depended on C–C coupling to provide additional phenyl or acetyl moieties to increase the length of the linker.[6, 17] Few studies, however, have looked to use shorter tetratopic linkers and thereby contract the framework.

Herein, the synthesis and characterization of a new *ftw* MOF, **NU-1106** ($Zr_6(\mu_3\text{-}O)_4(\mu_3\text{-}OH)_4(PyTC)_3$), is described, where $PyTC^{4-}$ is 1,3,6,8-pyrene tetracarboxylate. Due to its *ftw* topology, **NU-1106** has a cubic pore of approximately 10 Å

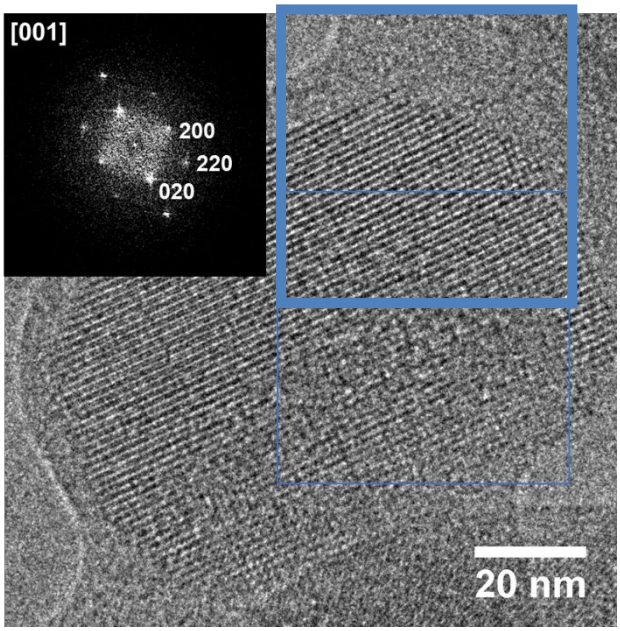

diameter, *i.e.* much smaller than previously synthesized **NU-110X** MOFs. The pyrene linker was synthesized using a new method to convert the tetrabromo-pyrene to the carboxylate (Fig. S1).[23] The new synthetic route for $PyTC^{4-}$ can be generalized for aryl halides as a tool for the development of new MOF linkers.[24]

The powdered X-ray diffraction (PXRD) of the MOF matches well with the simulated diffraction pattern of a previously reported Zr-based *ftw* MOF,[25] suggesting an isoreticular structure of **NU-1106** with *ftw* topology (Fig. S6). High resolution transmission electron microscopy (HR-TEM), a powerful tool that can discern the arrangement and separation distances of the dense Zr_6-clusters,[26, 27] was employed to confirm the structure of the MOF. Corresponding to the MOF tilted onto its crystallographic axis, it is observed that the 90° angle between diffraction patterns and the lattice spacing depict a MOF with *ftw* topology (Fig. 3).

Initial estimations projected that the aperture size of **NU-1106** to be approximately 3.0 Å (Fig. 2d). However, after synthesizing the sample, it was determined that N_2, which has a kinetic diameter of 3.6 Å, can be adsorbed within the framework, revealing a BET area of 355 m^2/g from the N_2 isotherm at 77 K. To interrogate this behaviour further, ^1H NMR of the digested MOF and thermogravimetric analysis (TGA) were used to estimate the number of defects within the system. According to TGA data obtained, **NU-1106** experienced approximately 50% mass loss after 410 °C (Fig. S5).

Figure 3. HR-TEM of NU-1106. Inset depicts the diffraction taken from within the blue square.

Extrapolating from this data, there were approximately 2 linkers per Zr_6 node, or about 25% missing linker within the MOFs when compared to the

Table 1. Xe uptake and Henry's Selectivity of MOFs

Adsorbent	*Xe Uptake (cm^3/g @ 1 bar)*	*Henry's Selectivity*
UiO-66[28]	35	7.2
HKUST-1[29]	70	8.5
MIL-101 (Cr)[28]	30	5.3
MIL-100 (Fe)[28]	26	5.6
NU-1106	**38**	**~10**

expected chemical formula. Since the MOF synthesis occurred in the presence of formic acid, ^{1}H-NMR of digested MOF was examined to further investigate the presence of defects. Formates act as monotopic ligands that coordinate to the Zr-node and reduce possible linker connectivity.[30] The NMR spectrum of **NU-1106** revealed a mole ratio of 1.3 formates per linker (Fig. S2), which corresponds to a minimum of about 33% missing linkers. The defect densities estimated through TGA and NMR are similar and indicate a highly defective MOF.

A primary reason for using Zr-based MOFs for gas and chemical separations is due to their overall stability. To investigate the thermal stability of **NU-1106** further, *in situ* PXRD was used to monitor the MOF's crystallinity under increasing temperatures (Fig. 2a). Starting at 150 °C, temperatures were held constant for one hour with measurements taken every 6 minutes. Measurements were collected every 10 °C until total crystallinity loss was observed. As indicated by the decrease in absolute intensity, experiments revealed a significant loss of crystallinity starting at 340 °C. Complete loss of crystallinity occurred at 370 °C, slightly lower than the decomposition temperature suggested by TGA (Fig 2a). The different materials developed for separations need to withstand degradation under harsh conditions. PXRD experiments were also used to determine MOF stability in the presence of water and confirmed that the MOF retained its structural integrity, even when immersed in water at 80 °C for 24 hrs and at room temperature for 2 weeks (Fig. S6).

Recent advances in the separation of Xe/Kr have been observed using MOFs. Initial efforts exploited the greater polarizability of Xe over Kr by adding polarizable functionalities to robust frameworks.[31, 32] Molecular simulations by Anderson *et al.* further demonstrated the need for a rigid structure and a pore-size that does not inhibit the diffusion of Xe or compromise on the confinement effect.[33] Due to its overall compactness, **NU-1106** showed potential over previous *ftw* MOFs for Xe/Kr separation. Delocalized electron clouds present on the pyrene linker can interact with the more polarizable Xe over Kr.[34, 35] Most importantly, the defects that permit nitrogen uptake also permit the uptake of both Xe and Kr.[36, 37]

The biphenyl derivative of the Zr-based *ftw* MOF[25] (530 m^2/g) was synthesized and compared with the adsorption capabilities of **NU-1106**. For both MOFs, Xe and Kr isotherms were taken at room-temperature. From the isotherms, both Xe and Kr show greater adsorption at 1 bar in **NU-1106** (Fig. 2b, 2c).

The uptake of Xe in **NU-1106** (38 cm^3/g) is higher than that of the biphenyl version (16 cm^3/g) and follows a similar trend for Kr uptake. By comparing **NU-1106** to the biphenyl derivative, it is understood that the higher uptake is due to greater polarizability of Xe and its interaction with a more complex π system of the pyrene versus the biphenyl. The Henry's selectivity for the pyrene MOF (~10) is nearly double that of the biphenyl MOF (5.6) and compares favourably to other common MOF adsorbents – including UiO-66, HKUST-1, MIL-100 (Fe) and MIL-101 (Cr) – tested for Xe/Kr selectivity (Table 1).

Conclusions

Developing methods to improve isoreticular synthesis in MOFs could better demonstrate strategies for enhancing specific MOF functions, especially gas separation. Characterization of **NU-1106** revealed a thermally stable MOF that remained crystalline in the presence of water. Restricting the linker length and increasing its bulkiness confines the pore while maintaining storage capacity, which enables for the selectivity of the more polarizable Xe over Kr. Going forward, we are developing a synthetic strategy for minimally defective **NU-1106** which can be useful for different separations that require small pore apertures.

Conflicts of interest

There are no conflicts to declare.

Acknowledgments

The authors gratefully acknowledge support from the U.S. Department of Energy (DOE) Office of Science, Basic Energy Sciences Program for Separation (DE-FG02-08ER15967). This work made use of the EPIC facility of Northwestern University's NUANCE Center, which has received support from the Soft and Hybrid Nanotechnology Experimental (SHyNE) Resource (NSF NNCI-1542205); the MRSEC program (NSF DMR1720139) at the Materials Research Center; the Army Research Office (W911NF1810359); the Keck Foundation; the International Institute for Nanotechnology (IIN); and the State of Illinois through the IIN. This work made use of the IMSERC at Northwestern University, which has received support from the NSF (CHE-1048773 and DMR0521267); the SHyNE Resource (NSF NNCI-1542205); the State of Illinois, and the IIN.

Notes and references

1. D. S. Sholl and R. P. Lively, *Nature*, 2016, **532**, 435-438.
2. K. Adil, Y. Belmabkhout, R. S. Pillai, A. Cadiau, P. M. Bhatt, A. H. Assen, G. Maurin and M. Eddaoudi, *Chem Soc Rev*, 2017, **46**, 3402-3430.
3. D. Banerjee, A. J. Cairns, J. Liu, R. K. Motkuri, S. K. Nune, C. A. Fernandez, R. Krishna, D. M. Strachan and P. K. Thallapally, *Acc Chem Res*, 2015, **48**, 211-219.
4. S. T. Meek, S. L. Teich-McGoldrick, J. J. Perry, J. A.

Greathouse and M. D. Allendorf, *The Journal of Physical Chemistry C*, 2012, **116**, 19765-19772.
5. D. Banerjee, C. M. Simon, S. K. Elsaidi, M. Haranczyk and P. K. Thallapally, *Chem*, 2018, **4**, 466-494.
6. P. Deria, D. A. Gomez-Gualdron, W. Bury, H. T. Schaef, T. C. Wang, P. K. Thallapally, A. A. Sarjeant, R. Q. Snurr, J. T. Hupp and O. K. Farha, *J Am Chem Soc*, 2015, **137**, 13183-13190.
7. O. V. Gutov, W. Bury, D. A. Gomez-Gualdron, V. Krungleviciute, D. Fairen-Jimenez, J. E. Mondloch, A. A. Sarjeant, S. S. Al-Juaid, R. Q. Snurr, J. T. Hupp, T. Yildirim and O. K. Farha, *Chemistry*, 2014, **20**, 12389-12393.
8. S. J. Garibay and S. M. Cohen, *Chem Commun (Camb)*, 2010, **46**, 7700-7702.
9. J. Lyu, X. Zhang, K. I. Otake, X. Wang, P. Li, Z. Li, Z. Chen, Y. Zhang, M. C. Wasson, Y. Yang, P. Bai, X. Guo, T. Islamoglu and O. K. Farha, *Chem Sci*, 2019, **10**, 1186-1192.
10. F. Vermoortele, B. Bueken, G. Le Bars, B. Van de Voorde, M. Vandichel, K. Houthoofd, A. Vimont, M. Daturi, M. Waroquier, V. Van Speybroeck, C. Kirschhock and D. E. De Vos, *J Am Chem Soc*, 2013, **135**, 11465-11468.
11. X. Wang, X. Zhang, P. Li, K.-i. Otake, Y. Cui, J. Lyu, M. D. Krzyaniak, Y. Zhang, Z. Li, J. Liu, C. T. Buru, T. Islamoglu, M. R. Wasielewski, Z. Li and O. K. Farha, *J. Am. Chem. Soc.*, 2019, **141**, 8306-8314.
12. R. J. Drout, A. J. Howarth, K.-i. Otake, T. Islamoglu and O. K. Farha, *CrystEngComm*, 2018, **20**, 6140-6145.
13. S. Rangwani, A. J. Howarth, M. R. DeStefano, C. D. Malliakas, A. E. Platero-Prats, K. W. Chapman and O. K. Farha, *Polyhedron*, 2018, **151**, 338-343.
14. X. Lian, Y. P. Chen, T. F. Liu and H. C. Zhou, *Chem Sci*, 2016, **7**, 6969-6973.
15. P. Li, Q. Chen, T. C. Wang, N. A. Vermeulen, B. L. Mehdi, A. Dohnalkova, N. D. Browning, D. Shen, R. Anderson, D. A. Gómez-Gualdrón, F. M. Cetin, J. Jagiello, A. M. Asiri, J. F. Stoddart and O. K. Farha, *Chem*, 2018, **4**, 1022-1034.
16. Y. Chen, P. Li, J. Zhou, C. T. Buru, L. Đorđević, P. Li, X. Zhang, M. M. Cetin, J. F. Stoddart, S. I. Stupp, M. R. Wasielewski and O. K. Farha, *J. Am. Chem. Soc.*, 2020, DOI: 10.1021/jacs.9b12828.
17. T. C. Wang, W. Bury, D. A. Gomez-Gualdron, N. A. Vermeulen, J. E. Mondloch, P. Deria, K. Zhang, P. Z. Moghadam, A. A. Sarjeant, R. Q. Snurr, J. F. Stoddart, J. T. Hupp and O. K. Farha, *J Am Chem Soc*, 2015, **137**, 3585-3591.
18. Y. Zhang, X. Zhang, J. Lyu, K. I. Otake, X. Wang, L. R. Redfern, C. D. Malliakas, Z. Li, T. Islamoglu, B. Wang and O. K. Farha, *J. Am. Chem. Soc.*, 2018, **140**, 11179-11183.
19. J. H. Cavka, S. Jakobsen, U. Olsbye, N. Guillou, C. Lamberti, S. Bordiga and K. P. Lillerud, *J. Am. Chem. Soc.*, 2008, **130**, 13850-13851.
20. H. Deng, S. Grunder, K. E. Cordova, C. Valente, H. Furukawa, M. Hmadeh, F. Gándara, A. C. Whalley, Z. Liu, S. Asahina, H. Kazumori, M. O'Keeffe, O. Terasaki, J. F. Stoddart and O. M. Yaghi, *Science*, 2012, **336**, 1018-1023.
21. H. Furukawa, Y. B. Go, N. Ko, Y. K. Park, F. J. Uribe-Romo, J. Kim, M. O'Keeffe and O. M. Yaghi, *Inorg. Chem.*, 2011, **50**, 9147-9152.
22. G. E. M. Schukraft, S. Ayala, B. L. Dick and S. M. Cohen, *Chem. Commun.*, 2017, **53**, 10684-10687.
23. T. Ueda, H. Konishi and K. Manabe, *Org Let*, 2013, **15**, 5370-5373.
24. X. Zhang, Z. Huang, M. Ferrandon, D. Yang, L. Robison, P. Li, T. C. Wang, M. Delferro and O. K. Farha, *Nat. Catal.*, 2018, **1**, 356-362.
25. H. Wang, X. Dong, J. Lin, S. J. Teat, S. Jensen, J. Cure, E. V. Alexandrov, Q. Xia, K. Tan, Q. Wang, D. H. Olson, D. M. Proserpio, Y. J. Chabal, T. Thonhauser, J. Sun, Y. Han and J. Li, *Nat. Commun.*, 2018, **9**, 1745.
26. Y. Zhu, J. Ciston, B. Zheng, X. Miao, C. Czarnik, Y. Pan, R. Sougrat, Z. Lai, C. Hsiung, K. Yao, I. Pinnau, P. Ming and Y. Han, *Nat Mater*, 2017, **16**, 532-537.
27. X. Gong, H. Noh, N. C. Gianneschi and O. K. Farha, *J Am Chem Soc*, 2019, **141**, 6146-6151.
28. S. J. Lee, T. U. Yoon, A. R. Kim, S. Y. Kim, K. H. Cho, Y. K. Hwang, J. W. Yeon and Y. S. Bae, *J Hazard Mater*, 2016, **320**, 513-520.
29. A. Soleimani Dorcheh, D. Denysenko, D. Volkmer, W. Donner and M. Hirscher, *Microporous and Mesoporous Materials*, 2012, **162**, 64-68.
30. W. Liang, C. J. Coghlan, F. Ragon, M. Rubio-Martinez, D. M. D'Alessandro and R. Babarao, *Dalton Trans*, 2016, **45**, 4496-4500.
31. O. V. Magdysyuk, F. Adams, H. P. Liermann, I. Spanopoulos, P. N. Trikalitis, M. Hirscher, R. E. Morris, M. J. Duncan, L. J. McCormick and R. E. Dinnebier, *Phys Chem Chem Phys*, 2014, **16**, 23908-23914.
32. Y.-S. Bae, B. G. Hauser, Y. J. Colón, J. T. Hupp, O. K. Farha and R. Q. Snurr, *Microporous and Mesoporous Materials*, 2013, **169**, 176-179.
33. R. Anderson, B. Schweitzer, T. Wu, M. A. Carreon and D. A. Gomez-Gualdron, *ACS Appl Mater Interfaces*, 2018, **10**, 582-592.
34. X. Chen, A. M. Plonka, D. Banerjee, R. Krishna, H. T. Schaef, S. Ghose, P. K. Thallapally and J. B. Parise, *J Am Chem Soc*, 2015, **137**, 7007-7010.
35. D. Banerjee, C. M. Simon, A. M. Plonka, R. K. Motkuri, J. Liu, X. Chen, B. Smit, J. B. Parise, M. Haranczyk and P. K. Thallapally, *Nat Commun*, 2016, **7**, ncomms11831.
36. K. Wang, C. Li, Y. Liang, T. Han, H. Huang, Q. Yang, D. Liu and C. Zhong, *Chemical Engineering Journal*, 2016, **289**, 486-493.
37. P. Iacomi, F. Formalik, J. Marreiros, J. Shang, J. Rogacka, A. Mohmeyer, P. Behrens, R. Ameloot, B. Kuchta and P. L. Llewellyn, *Chemistry of Materials*, 2019, **31**, 8413-8423.